Controlling Vesicle Formation via Interpolymer Hydrogen-Bonding Complexation between Poly(ethylene oxide)-*block*-polybutadiene and Poly(acrylic acid) in Solution

Wei-Ping Gao,[†] Yu Bai,[†] Er-Qiang Chen,*[,†] Zi-Chen Li,*[,†] Bing-Yong Han,[‡] Wan-Tai Yang,[‡] and Qi-Feng Zhou*[,†]

Department of Polymer Science and Engineering and The Key Laboratory of Polymer Chemistry and Physics of the Ministry of Education, College of Chemistry and Molecular Engineering, Peking University, Beijing 100871, China, and College of Material Science and Engineering, Beijing University of Chemical Technology, Beijing 100029, China

Received February 17, 2006; Revised Manuscript Received April 28, 2006

ABSTRACT: This paper describes a controllable vesicle formation of a diblock copolymer of poly(ethylene oxide)-*block*-polybutadiene (PEO-*b*-PB) and a homopolymer of poly(acrylic acid) (PAA) in a solvent mixture of THF and *n*-dodecane. The number-average molecular weights (M_n) of both the PEO and PB blocks are 5100 g/mol; the weight-average molecular weight (M_w) of the PAA is ∼2000 g/mol. The assembly is driven by the hydrogen-bonding complexation between the complementary binding sites on PEO and PAA. The vesicles can load PAA far above the stoichiometrical monomer ratio of PAA to PEO ([AA]/[EO]). At $0.85 \leq$ [AA]/[EO] ≤ 2.5, unilamellar vesicles (ULVs) with a constant membrane thickness of 16 nm are obtained in a controllable manner, of which the surface area increases linearly with [AA]/[EO]. Further increasing [AA]/[EO] above 3 results in the formation of multivesicular vesicles (MVVs). The PAA chains in ULVs are uniformly inserted into membranes with a direction preferentially perpendicular to the interface. When the PB blocks are unable to sufficiently cover the interface and the PEO blocks do not interact homogeneously with PAA chains, the MVVs form.

Introduction

Block copolymers in the solvents that are selective for one of the blocks may exhibit fascinating self-assembly behaviors,[1] wherein spherical and cylindrical micelles, lamellae, and vesicles are usually observed. Of particular interest is how to control the polymer assembly in solutions. Thermodynamically, the delicate balance among the interfacial energy of the soluble/insoluble interface, intercoronal chain interactions, and entropy loss due to the insoluble blocks packed into aggregate microdomains determines the final structure of assemblies. Therefore, the effective ways to modulate the balance include varying chemical structures, compositions, and architectures of copolymers[2−9] and the solution conditions (concentration, temperature, solubility, pH, ionic strength, etc.).[10] Recent advancement has demonstrated that the interpolymer complexation can also induce polymer assembly in solutions.[11−13] An interpolymer complexation can change significantly in terms of the polymer solubility and conformation, which facilitates the intercomplex aggregation.[14] The interactions can be electrostatic interaction,[11] hydrogen bonding,[11f,12] metal−ligand coordination bond,[12a,13] etc. Obviously, taking advantage of such strong secondary interactions, one may greatly enhance the ability toward manipulating novel and well-defined ordered structures in a nanometer scale and explore considerable potentials amenable to practical applications.

In this study, we report the vesicle formation[15] in a blend solution containing a diblock copolymer of poly(ethylene oxide)-*block*-polybutadiene (PEO-*b*-PB) and a homopolymer of low molecular weight poly(acrylic acid) (PAA). The assembly is driven by the hydrogen-bonding complexation between the complementary binding sites on PEO and PAA. Such complexation has been well studied,[14] yet remains as an interesting topic so far.[16] In the PEO/PAA solution and solid state as well, a stoichiometrical process with the molar ratio of the two repeating units, [AA]/[EO], close to 1 was identified.[14] Therefore, one can expect that the interpolymer hydrogen bonding between PAA and PEO-*b*-PB will readily lead to some sort of supramolecular assembly (which is vesicle here) around the stoichiometrical point. Interestingly, our blend system presents unilamellar vesicles (ULVs) when [AA]/[EO] varies from 0.8 to 2.5. At a higher [AA]/[EO], multivesicular vesicles (MVVs) appear, where many nonconcentric small (daughter) vesicles reside in a much large (mother) one.[17] Combining the dynamic light scattering (DLS) and transmission electron microscopy (TEM), we quantitatively describe the vesicle morphology change as a function of the PAA content. The work is concerned with where the PAA chains are accommodated and at what condition the ULVs are stable.

Experimental Section

The detailed synthetic procedure and the chemical characterization of the PEO-*b*-PB diblock copolymer were reported elsewhere.[18] The PB block was obtained through the anionic polymerization of butadiene in cyclohexane using *n*-butyllithium as the initiator and thus is 1,4-structure dominant. The diblock copolymer possesses a number-average molecular weight (M_n, measured by ^{1}H NMR, Bruker ARX400 spectrometer) of 5100 g/mol for both the PEO and PB blocks, and its polydispersity (M_w/M_n, measured by GPC, Waters 150) is 1.06. The PAA with a weight-average molecular weight (M_w) of ∼2000 g/mol was purchased from Aldrich and was used as received. To obtain the solution assembly of the PEO-*b*-PB and PAA, the two polymers were first dissolved in a common solvent of THF, with an initial diblock concentration of

[†] Peking University.
[‡] Beijing University of Chemical Technology.
* To whom correspondence should be addressed. E-mail: eqchen@pku.edu.cn; zcli@pku.edu.cn; qfzhou@pku.edu.cn.

10.1021/ma0603579 CCC: $33.50
Published on Web 06/07/2006

2.5 mg/mL. The weight ratio of the PAA/PEO-*b*-PB (W_A/W_{EB}) ranged from 0.7 to 10, i.e., [AA]/[EO] from 0.85 to 12.2 ([AA]/[EO] $\approx$ (W_A/72)/(0.5 $\times$ W_{EB}/44), where 72 and 44 are the molar masses of the repeating units of PAA and PEO and 0.5 is the weight fraction of the PEO in the diblock). Under moderate mechanical stirring, *n*-dodecane, a selective solvent for PB but a poor solvent for both PEO and PAA, was then gradually dropped into the clear solution until the volume ratio of *n*-dodecane/THF (v/v) reached 10:1. The mixture was stirred for more than 24 h at room temperature. For comparison, we also added *n*-dodecane to the THF solutions of the pure PAA and PEO-*b*-PB with the concentrations of 2.5 mg/mL.

DLS experiments were performed with a spectrometer (ALV/DLS/SLS-5022F) equipped with a multi-τ digital time correlation (ALV5000) and a cylindrical 22 mW uniphase He−Ne laser (λ_0 = 632 nm). All measurements were carried out at 25 °C, with a detection angle of 90°. Before mixing, the THF solutions of PAA/PEO-*b*-PB and *n*-dodecane were filtered through 0.45 μm Millipore filters. The viscosity (η) and refractive index (n) of *n*-dodecane/THF (v/v 10:1) were measured to be 1.174 cP and 1.419, respectively. The scattering intensity autocorrelation functions were analyzed by using the methods of Contin and Cumulant.

TEM experiments were performed using a JEM-200CX microscope with an accelerating voltage of 120 kV. The samples for TEM were prepared by depositing the blend solutions onto copper grids that were precoated with a thin film of Formvar and then coated with carbon, which were dried freely at ambient conditions followed by in a vacuum for days. Some samples were stained with OsO_4 vapor for 8 min before examined under TEM.

Results and Discussion

When *n*-dodecane was added into the THF solution of the pure PAA, the PAA was easily precipitated out at *n*-dodecane/THF (v/v) of around 1:2. In contrast, the addition of *n*-dodecane made the blend solutions of the PAA/PEO-*b*-PB become bluish at *n*-dodecane/THF (v/v) of 10:1. For $W_A/W_{EB} \leq 3$, the bluish solutions were stable for over months. When $3 < W_A/W_{EB} < 8$, only trace amounts of white precipitates appeared 48 h later after the stir was stopped. If $W_A/W_{EB} \geq 8$, the precipitation from the bluish solutions became obvious. The bluish hue of the blend solutions implies that the PAA chains have incorporated with the PEO-*b*-PB diblocks to form small aggregates. Since *n*-dodecane is a selective solvent for PB, the aggregates should comprise the shells of soluble PB blocks and the dense insoluble cores of the mixed PEO and PAA. In the THF solutions, the hydrogen bonding between the PAA and PEO block may not exist as THF destroys the interaction. Adding *n*-dodecane can progressively turn the medium to be poorer and eventually lead to coprecipitation of the PAA and PEO forming the cores of the aggregates. We consider that the coprecipitation can arise from the interpolymer hydrogen bonding. Our FT-IR experiments confirmed that the hydrogen bonding between the ether oxygens of PEO blocks and the carboxylic acid groups of PAA existed in the solid state of the PAA/PEO-*b*-PB blend. Compared with the pure PEO-*b*-PB, the $\nu(C-O-C)_{asym}$ band center of the PEO blocks in the mixture shifts from 1115 cm^{-1} to a lower wavenumber of 1105 cm^{-1}.[19a] On the other hand, the carbonyl absorption band of PAA at 1724 cm^{-1} in the mixture is 10 cm^{-1} higher than that in the pure PAA.[19b−d]

The small aggregates in the blend solutions with $W_A/W_{EB} \leq 3.0$ were investigated via DLS at room temperature. Figure 1 illustrates the apparent hydrodynamic radius (R_h) distributions of the PAA/PEO-*b*-PB aggregates as a function of W_A/W_{EB}. For comparison, Figure 1 also includes the DLS result of the pure PEO-*b*-PB in the *n*-dodecane/THF (v/v = 10:1). For each blend solution, the size distribution consists of a single peak with a relative line width (μ_2/Γ^2) smaller than 0.1. The unimers of the diblock copolymer and the PAA with R_hs smaller than 10 nm were not detected, indicating that most polymers are incorporated into the aggregates. The narrow size distribution further implies the well-defined structures of the small aggregates. While the pure PEO-*b*-PB gives the peak position of R_h at 20 nm, the blend solutions present much larger R_hs around 100 nm. Moreover, the peak of the blend solution shifts monotonically toward higher R_h with the increasing PAA content (also see Table 1).

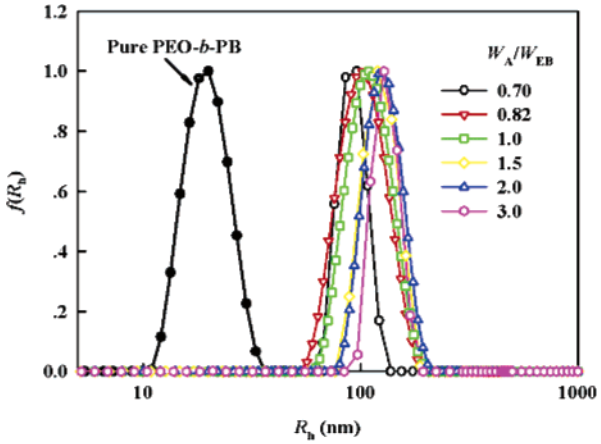

Figure 1. Hydrodynamic radius distributions ($f(R_h)$) of the PAA/PEO-*b*-PB in *n*-dodecane/THF (v/v = 10:1) at different values of W_A/W_{EB}. The $f(R_h)$ of the pure PEO-*b*-PB is also shown.

Table 1. R_h, N_{EB}, and s at Different W_A/W_{EB}s

W_A/W_{EB}	0.70	0.82	1.0	1.5	2.0	3.0
[AA]/[EO]	0.85	1.00	1.22	1.83	2.44	3.67
R_h (nm)	100	102	109	122	127	131
N_{EB} ($\times 10^{-4}$)[a]	5.9	5.7	6.0	6.1	5.6	4.5
s (nm^2/block)[b]	3.60	3.85	4.23	5.29	6.35	8.47

[a] N_{EB} = the average number of PEO-*b*-PB molecules per vesicle, calculated by eq 1a. [b] s = the average surface area per PB block, calculated by eq 2. M_{EB} is 10 200 g/mol, L is 16 nm, and ρ is assumed to be 1 g/cm^3.

The morphology of the assemblies was examined under TEM after the complete removal of solvents. The pure PEO-*b*-PB formed spherical micelles in the solvent mixture (see Supporting Information), but the morphology of ULV was observed for the blend solutions at $0.7 \leq W_A/W_{EB} \leq 2$. Figure 2a presents a pristine TEM image with W_A/W_{EB} = 0.70. The vesicular structure is evidenced from a higher transmission in the center of the aggregates than around their periphery. For more structure details, Figure 2b of W_A/W_{EB} = 2.0 shows a typical morphology of ULVs after stained by OsO_4 vapor. Since OsO_4 stains the PB blocks more heavily due to the presence of unsaturation, the outer and inner PB layers of the vesicular membranes look darker than the cores of PAA/PEO complexes. The membrane possesses an overall thickness (L) of ~16 nm, wherein the core is nearly 8 nm. As the PEO blocks with M_n = 5100 g/mol has an unperturbed end-to-end distance (r_0) of ~4 nm, the core thickness of 8 nm indicates that the membrane is a bilayer or a partially interdigitated structure with the PEO blocks extended to a certain extent when the PAA/PEO complexation is formed. Our TEM results have confirmed that the vesicle size increases when W_A/W_{EB} changes from 0.70 to 2.0. However, the L remains nearly constant at 16 nm.

For the stoichiometric mixture of the PAA and PEO, a fair long continuous linear succession of hydrogen bonds between monomer units of the PAA and PEO may result in a ladderlike structure. According to Antonietti and Förster,[15b] such a complexation will restrict the intermolecular conformation and lead to a preferred parallel alignment, facilitating the formation

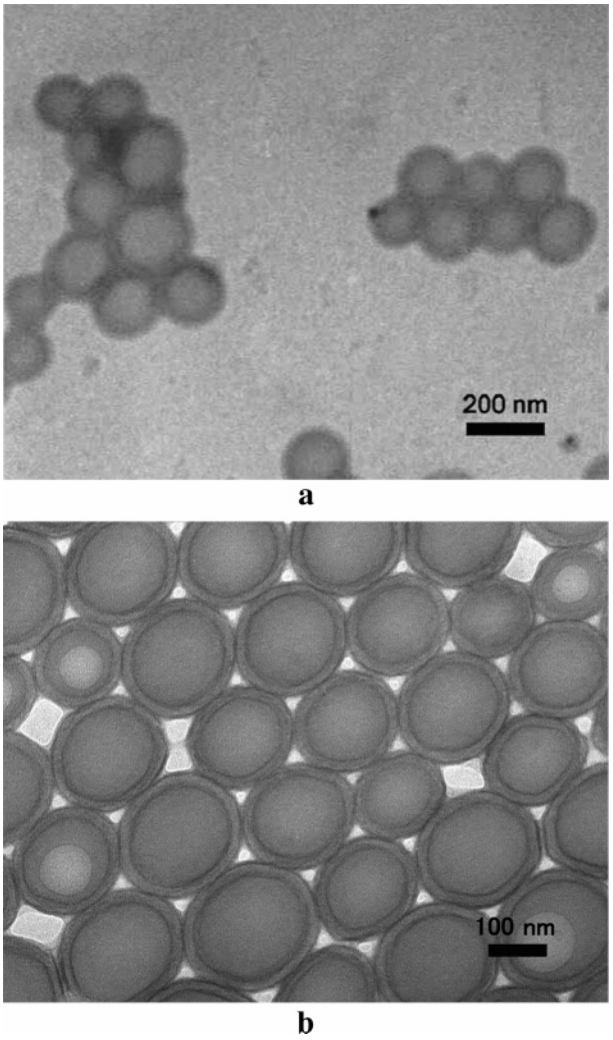

Figure 2. Typical TEM images of PAA/PEO-*b*-PB ULVs: (a) pristine sample of $W_A/W_{EB} = 0.7$; (b) OsO_4 stained sample of $W_A/W_{EB} = 2.0$.

of vesicles. It is of interest to find how the PAA chains are incorporated into the vesicles at [AA]/[EO] above the stoichiometrical point. One may speculate that the excess PAA chains are accommodated at the center portions of membranes. In this case, the membrane thickness will increase with the PAA content, but our experimental observation of the constant L of ULVs precludes this possibility. Most likely, the PAA chains are uniformly inserted into the membrane cores with a direction more or less perpendicular to the interface. Frank et al. reported that, in aqueous solutions of the PEO and PAA with the molecular weights similar to our samples, the aggregation of PEO along PAA occurred in a homogeneous way until [AA]/[EO] = 2−3.[16a] For the ULVs in this study, we consider that the PEO blocks in the membranes also interact homogeneously with the surrounding PAA chains.

Figure 3 depicts a schematic draw of a bilayer ULV with a constant L. We assume that the average number of PEO-*b*-PB molecules per vesicle (N_{EB}) is simply equal to the ratio of the total number of the diblock molecules (i.e., $N_A W_{EB}/M_{EB}$) to the total number of the vesicles (N_v), where N_A and M_{EB} are Avogadro's number and molar mass of the PEO-*b*-PB, respectively. The radius of outer periphery (R in Figure 3) can be represented by the R_h at the peak position measured by DLS. Since L is much smaller than R, we take $4\pi(R_h - L/2)^2 L$ as an approximation to the vesicle volume and calculate $N_v = (W_A + W_{EB})/[4\pi(R_h - L/2)^2 L\rho]$, where ρ is the density of the

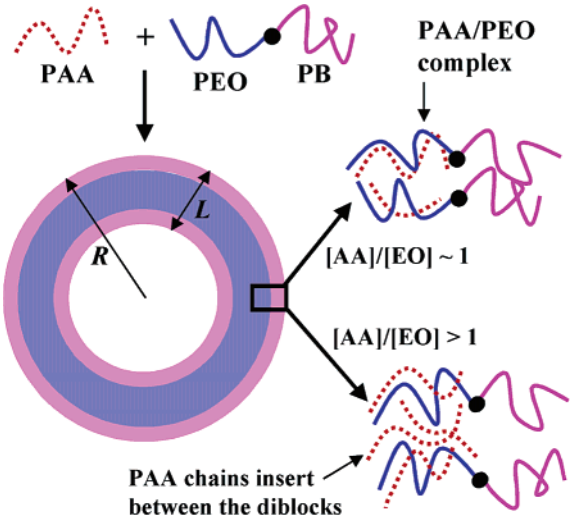

Figure 3. Schematic illustration of a bilayer ULV of PAA/PEO-*b*-PB. When [AA]/[EO] > 1, the excess PAA chains are uniformly inserted into the membrane core between the diblocks.

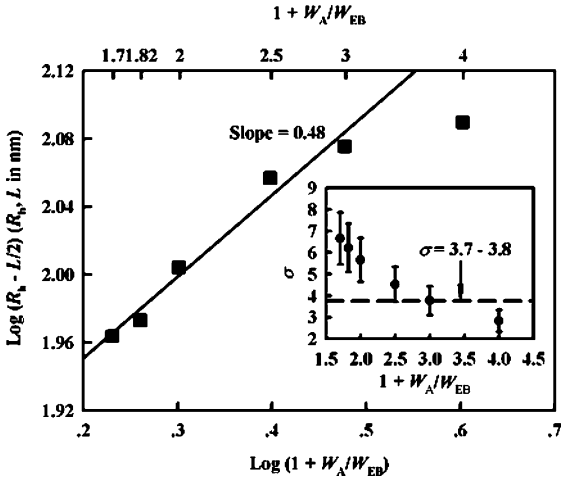

Figure 4. Double-logarithmic plot of $(R_h - L/2)$ vs $(1 + W_A/W_{EB})$. The inset shows the reduced tethering density (σ) of PB as a function of W_A/W_{EB}.

membrane that is close to 1 g/cm^3. Accordingly, we have

$$N_{EB} = \frac{N_A W_{EB}}{M_{EB} N_V} \approx \frac{N_A}{M_{EB}} \frac{4\pi(R_h - L/2)^2 L\rho}{1 + W_A/W_{EB}} \quad (1a)$$

$$R_h - L/2 \approx \left(\frac{N_{EB}}{C}\right)^{1/2} \left(1 + \frac{W_A}{W_{EB}}\right)^{1/2} \quad (1b)$$

where $C = 4\pi N_A L\rho/M_{EB}$ is nearly a constant. Figure 4 presents a double-logarithmic plot of $(R_h - L/2)$ vs $(1 + W_A/W_{EB})$. Up to $W_A/W_{EB} = 2.0$, the linear line representing a least-squares fitting yields a slope of 0.48, close to the theoretical datum of 0.5. This manifests that the surface area of ULVs is linearly proportional to W_A/W_{EB}, i.e., [AA]/[EO]. Furthermore, the N_{EB} should be almost a constant. The calculated values of N_{EB} shown in Table 1 are indeed close to each other when W_{AA}/W_{EB} varies from 0.7 to 2. The results suggest that the vesicle formation might be close to equilibrium, which can be attributed to the balance between the mixing entropy that favors more vesicles and the molar bending energy that tends to reduce the vesicle numbers.[15b]

As we fix the initial concentration of the diblock copolymer, the constant N_{EB} indicates that N_v should be also a constant

(see eq 1a). When more PAA chains insert into the ULV with N_{EB}, the average surface area per PB block (s) will increase, resulting in a larger vesicle radius. The relationship between s and PAA content is rather simple:

$$s \approx 2\frac{4\pi(R_h - L/2)^2}{N_{EB}} = 2\frac{M_{EB}}{N_A L\rho}\left(1 + \frac{W_A}{W_{EB}}\right) \qquad (2)$$

where the prefactor 2 counts the two surfaces of the membrane, and $(2M_{EB})/(N_A L\rho)$, in fact, is the value of s if the pure PEO-*b*-PB forms a bilayer lamella with the thickness of L. The calculated s is also listed in Table 1. The linear relationship in eq 2 makes our system different from the core−shell structures of microemulsion or spherical latex particles, where s is a constant.[20] We consider that s is one of the key factors that determines whether a ULV can be stabilized. When s increases, the PB blocks in the shell may undergo a conformation change from "brushes" to "mushrooms". It is reported recently, for polymer chains tethered on a lamellar surface, the onset of chain overcrowding in solution occurs at a critical value of the reduced tethering density (σ) of 3.7−3.8.[21] The reduced tethering density is defined as $\sigma = \pi R_g^2/s$, where R_g is the radius of gyration of the soluble chains under specific experimental conditions. Since we do not have the exact R_g of the PB with $M_n = 5100$ g/mol in *n*-dodecane/THF (v/v = 10/1), we use the R_g of 2.5−3 nm to estimate the σ. The inset of Figure 4 presents the σ as a function of W_A/W_{EB}. For $W_A/W_{EB} \le 2$, the calculated σ exceeds the critical value proposed in ref 21. This implies that the PB blocks in shells are overcrowded and, therefore, can well protect the underneath PAA/PEO complexes. However, for $W_A/W_{EB} = 3.0$, the PB blocks enter the noninteracting ("mushrooms") regime. In this case, the s probably becomes too large to be fully covered by the PB blocks, making the ULVs unstable. This may be responsible for the deviation from the linear relationship at $W_A/W_{EB} = 3.0$ in Figure 4.

Another possible reason for the ULVs becoming unstable is that the PAA and PEO blocks are no longer mixed homogeneously at $W_A/W_{EB} > 2$, i.e., [AA]/[EO] > 2.5 in our system.[16a] As mentioned earlier, precipitates appeared from the solutions when W_A/W_{EB} exceeded 3, which might be pure PAA or some large aggregates of the PAA/PEO-*b*-PB that were kinetically trapped and could not retain longer in solutions (see Supporting Information). We therefore focus on the assemblies in the stable bluish solutions at $W_A/W_{EB} \ge 3$. As shown in Figure 5, the MVVs of the PAA/PEO-*b*-PB are observed. Such a vesicle structure can be formed in small molecular surfactants under certain experimental conditions,[17] but is few in polymer systems.[22] Figure 5a is a TEM image of the sample at $W_A/W_{EB} = 4$, illustrating the coexistence of ULVs with a few MVVs. With a continuously increased W_A/W_{EB}, the MVVs gradually become dominant (see Figure 5b of $W_A/W_{EB} = 10$ as an example). The mother vesicles of MVVs are 200−400 nm in diameter, with the membrane thickness of nearly 16 nm, similar to those found for $W_A/W_{EB} < 3$; the daughter vesicles are 50−70 nm in diameter, with membranes of around 12 nm thick. The thinner membranes seem to be more flexible, allowing the formation of smaller vesicles with a higher curvature. We currently do not fully understand the thermodynamics and mechanism of the MVV formation. We suspect that within the daughter vesicles the hydrogen bonding among PAA chains becomes important.[16e] As the MVVs only form at high W_A/W_{EB}, the daughter vesicles might be predominantly composed of PAA.

It is known that copolymer micelles in a selective solvent can load homopolymer that is miscible with the core-forming block but insoluble in the solvent. However, the weight fraction of homopolymer solubilized in micelles based on weak secondary interactions is no more than 100 wt %.[2b,23] Our experimental results reveal that, with the help of specific interaction of interpolymer hydrogen bonding, the resultant PAA/PEO-*b*-PB vesicles can load the PAA homopolymer in large amount. For the ULVs with a bilayer structure, the core thickness is mainly determined by the length of PEO blocks. We may expect that if longer PEO blocks are used to form thicker membrane cores, the ULVs will incorporate more PAA chains when the two complementary chains interact in a homogeneous way. On the other hand, according to the critical reduced tethering density argument, increasing the molecular weight (and thus increasing the R_g) of the PB blocks may also lead to more PAA chains inserted into the ULVs. Since the MVVs can form at high PAA content, the assembly of the PAA/PEO-*b*-PB demonstrates a greatly enhanced ability of loading PAA.

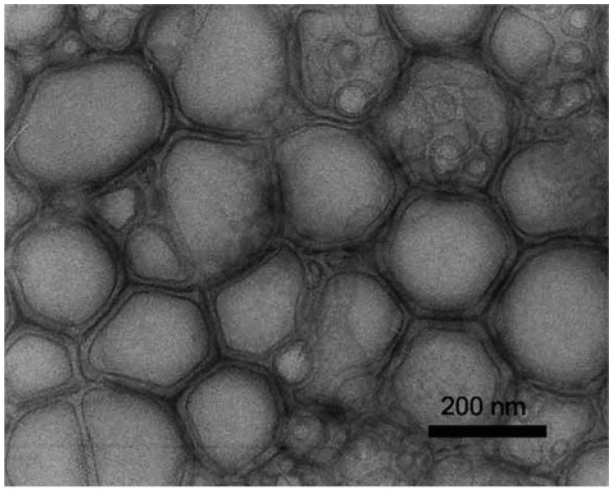

a

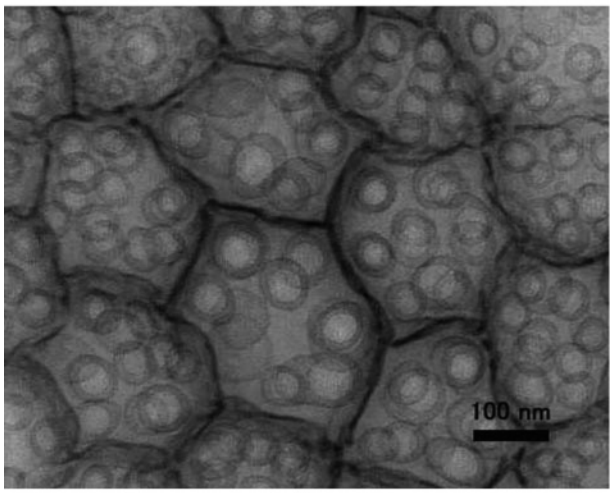

b

Figure 5. TEM images of OsO_4 stained samples obtained from the bluish solutions of W_A/W_{EB} at (a) 4.0 and (b) 10.0.

Summary

We have successfully induced the vesicle formation of the PAA/PEO-*b*-PB in solution based on the interpolymer hydrogen-bonding complexation between PAA and PEO. The vesicles can load PAA far above the stoichiometrical [AA]/[EO]. For $0.70 \le W_A/W_{EB} \le 2.0$, i.e., $0.8 \le$ [AA]/[EO] ≤ 2.5, the ULVs with membrane thickness of ∼16 nm are obtained in a controllable manner. The surface area of ULVs is linearly

proportional to W_A/W_{EB}. The excess PAA chains are uniformly inserted into membranes with a direction preferentially perpendicular to the interface, leading to the increase in the surface area per PB block. The ULVs are stable when the PB blocks tethered on the interface are overcrowded. When W_A/W_{EB} is above 2, the MVVs appear. We expect that tuning the sizes of PB and PEO blocks can be an effective way toward controlling the vesicles of PAA/PEO-*b*-PB. We also consider that the simple strategy of polymer vesicle formation reported here may provide a clue to explore possible applications in drug delivery systems, medical implantation, nanostructure fabrications, etc.

Acknowledgment. This work was supported by the National Natural Science Foundation of China (Grants 20025414, 20374003, and 50573001). We thank Prof. J.-B. Huang and Dr. S.-Q. Wang at Peking University and Prof. F. Qiu at Fudan University for useful suggestions.

Supporting Information Available: TEM images of spherical micelles of the pure PEO-*b*-PB and the larger aggregates of PAA/PEO-*b*-PB at $W_{AA}/W_{EO} > 3$. This material is available free of charge via the Internet at http://pubs.acs.org.

References and Notes

(1) Halperin, A.; Tirrell, M.; Lodge, T. P. *Adv. Polym. Sci.* **1992**, *100*, 31−71. (b) Tuzar, Z.; Kratochvil, P. In *Surface and Colloid Science*; Matijević, Ed.; Plenum: New York, 1993; Vol. 15, Chapter 1, pp 1−83. (c) Chu, B. *Langmuir* **1995**, *11*, 414−421. (d) Cameron, N. S.; Corbierre, M. K.; Eisenberg, A. *Can. J. Chem.* **1999**, *77*, 1311−1326. (e) Jain, S.; Bates, F. S. *Science* **2003**, *300*, 460−464.

(2) Zhang, L.; Eisenberg, A. *Science* **1995**, *268*, 1728−1731. (b) Zhang, L.; Eisenberg, A. *J. Am. Chem. Soc.* **1996**, *118*, 3168−3181. (c) Förster, S.; Zisenis, M.; Wenz, E.; Antonietti, M. *J. Chem. Phys.* **1996**, *104*, 9956−9970.

(3) van Hestm, J. C. M.; Delnoye, D. A. P.; Baars, M. W. P. L.; van Genderen, M. H. P.; Meijer, E. W. *Science* **1995**, *268*, 1592−1595.

(4) Jenekhe, S. A.; Chen, X. L. *Science* **1998**, *279*, 1903−1907. (b) Zubarev, E. R.; Pralle, M. U.; Sone, E. D.; Stupp, S. I. *J. Am. Chem. Soc.* **2001**, *123*, 4105−4106. (c) Tu, Y.; Wan, X.; Zhang, D.; Zhou, Q.; Wu, C. *J. Am. Chem. Soc.* **2000**, *122*, 10201−10205.

(5) Cornelissen, J. J. L. M.; Fischer, M.; N. Sommerdijk, A. J. M.; Nolte, R. J. M. *Science* **1998**, *280*, 1427−1430.

(6) Zhou, Z.; Li, Z.; Ren, Y.; Hillmyer, M. A.; Lodge, T. P. *J. Am. Chem. Soc.* **2003**, *125*, 10182−10183. (b) Li, Z.; Kesselman, E.; Talmon, Y.; Hillmyer, M. A.; Lodge, T. P. *Science* **2004**, *306*, 98−101.

(7) Yan, D.; Zhou, Y.; Hou, J. *Science* **2004**, *303*, 65−67.

(8) Massey, J. A.; Temple, K.; Cao, L.; Rharbi, Y.; Raez, J.; Winnik, M. A.; Manners, I. *J. Am. Chem. Soc.* **2000**, *122*, 11577−11584.

(9) Cheng, C.-X.; Huang, Y.; Tang, R.-P.; Chen, E.-Q.; Xi, F. *Macromolecules* **2005**, *38*, 3044−3047.

(10) Zhang, L.; Yu, K.; Eisenberg, A. *Science* **1996**, *272*, 1777−1779. (b) Yu, Y.; Zhang, L.; Eisenberg, A. *Macromolecules* **1998**, *31*, 1144−1154. (c) Iyama, K.; Nose, T. *Polymer* **1998**, *39*, 651−658. (d) Won, Y. Y.; Davis, H. T.; Bates, F. S. *Science* **1999**, *283*, 960−963. (e) Jain, S.; Bates, F. S. *Macromolecules* **2004**, *37*, 1511−1523. (f) Pochan, D. J.; Chen, Z.; Cui, H.; Hales, K.; Qi, K.; Wooley, K. L. *Science* **2004**, *306*, 94−97. (g) Gohy, J.-F.; Willet, N.; Varshney, S.; Zhang, J. X.; Jérôme, R. *Angew. Chem., Int. Ed.* **2001**, *40*, 3214−3216.

(11) Harada, A.; Kataoka, K. *Macromolecules* **1995**, *28*, 5294−5299. (b) Harada, A.; Kataoka, K. *Science* **1999**, *283*, 65−67. (c) Fukushima, S.; Miyata, K.; Nishiyama, N.; Kanayama, N.; Yamasaki, Y.; Kataoka, K. *J. Am. Chem. Soc.* **2005**, *127*, 2810−2811. (d) Kabanov, A. V.; Bronich, T. K.; Kabanov, V. A.; Yu, K.; Eisenberg, A. *J. Am. Chem. Soc.* **1998**, *120*, 9941−9942. (e) Zhou, S.; Chu, B. *Adv. Mater.* **2000**, *12*, 545−556. (f) Gohy, J.-F.; Varshney, S. K.; Jérôme, R. *Macromolecules* **2001**, *34*, 3361−3366. (g) Schrage, S.; Sigel, R.; Schlaad, H. *Macromolecules* **2003**, *36*, 1417−1420. (h) Weaver, J. V. M.; Armes, S. P.; Liu, S. *Macromolecules* **2003**, *36*, 9994−9998.

(12) Zhang, G. Z.; Liu, S.; Zhao, H.; Jiang, M. *Mater. Sci. Eng., C* **1999**, *10*, 155−158. (b) Liu, S.; Zhu, H.; Zhao, H.; Jiang, M.; Wu, C. *Langmuir* **2000**, *16*, 3712−3717. (c) Liu, X.; Jiang, M.; Yang, S.; Chen, M.; Chen, D.; Yang, C.; Wu, K. *Angew. Chem., Int. Ed.* **2002**, *41*, 2950−2953. (d) Chen, D.; Jiang, M. *Acc. Chem. Res.* **2005**, *38*, 494−502. (e) Ilhan, F.; Galow, T. H.; Gray, M.; Clavier, G.; Rotello, V. M. *J. Am. Chem. Soc.* **2000**, *122*, 5895−5896. (f) Percec, V.; Dulcey, A. E.; Balagurusamy, V. S. K.; Miura, Y.; Smidrkal, J.; Peterca, M.; Nummelin, S.; Edlund, U.; Hudson, S. D.; Heiney, P. A.; Duan, H.; Magonov, S. N.; Vinogradov, S. A. *Nature (London)* **2004**, *430*, 764−768. (g) Hu, J.; Liu, G. *Macromolecules* **2005**, *38*, 8058−8065. (h) Yan, X.; Liu, G.; Hu, J.; Willson, C. G. *Macromolecules* **2006**, *39*, 1906−1912.

(13) Gohy, J.-F.; Hofmeier, H.; Alexeev, A.; Schubert, U. S. *Macromol. Chem. Phys.* **2003**, *204*, 1524−1530. (b) Grubbs, R. B. *J. Polym. Sci., Part A: Polym. Chem.* **2005**, *43*, 4323−4336.

(14) Bekturov, E.; Bimendina, L. *Adv. Polym. Sci.* **1981**, *41*, 99−147. (b) Tsuchida, E.; Abe, K. *Adv. Polym. Sci.* **1982**, *45*, 1−119. (c) Jiang, M.; Li, M.; Xiang, M.; Zhou, H. *Adv. Polym. Sci.* **1999**, *146*, 121−196.

(15) Discher, D. E.; Eisenberg, A. *Science* **2002**, *297*, 967−973. (b) Antonietti, M.; Förster, S. *Adv. Mater.* **2003**, *15*, 1323−1333. (c) Kita-Tokarczyk, K.; Grumelard, J.; Haefele, T.; Meier, W. *Polymer* **2005**, *46*, 3540−3563. (d) Discher, B. M.; Won, Y.-Y.; Ege, D. S.; Lee, J. C.-M.; Bates, F. S.; Discher, D. E.; Hammer, D. A. *Science* **1999**, *284*, 1143−1146. (e) Liu, F.; Eisenberg, A. *J. Am. Chem. Soc.* **2003**, *125*, 15059−15064. (f) Maskos, M.; Harris, J. R. *Macromol. Rapid Commun.* **2001**, *22*, 271−273. (g) Zhou, Y.; Yan, D. *Angew. Chem., Int. Ed.* **2004**, *43*, 4896−4899.

(16) Oyama, H. T.; Tang, W. T.; Frank, C. W. *Macromolecules* **1987**, *20*, 474−480. (b) Hemker, D. J.; Garza, V.; Frank, C. W. *Macromolecules* **1990**, *23*, 4411−4418. (c) Miyoshi, T.; Takegoshi, K.; Hikichi, K. *Polymer* **1997**, *38*, 2315−2320. (d) Khutoryanskiy, V. V.; Dubolazov, A. V.; Nurkeeva, Z. S.; Mun, G. A. *Langmuir* **2004**, *20*, 3785−3790. (e) Lutkenhaus, J. L.; Hrabak, K. D.; McEnnis, K.; Hammond, P. T. *J. Am. Chem. Soc.* **2005**, *127*, 17228−17234.

(17) Walde, P.; Ichikawa, S. *Biomol. Eng.* **2001**, *18*, 143−177. (b) Menger, F. M.; Gabrielson, K. *J. Am. Chem. Soc.* **1994**, *116*, 1567−1568. (c) Menger, F. M.; Lee, S. J.; Keiper, J. S. *Langmuir* **1996**, *12*, 4479−4480.

(18) Gao, W.-P.; Bai, Y.; Chen, E.-Q.; Zhou, Q.-F. *Chin. J. Polym. Sci.* **2005**, *23*, 275−284.

(19) Kadla, J. F.; Kubo, S. *Macromolecules* **2003**, *36*, 7803−7811. (b) Macknight, W. J.; Mekenna, L. W.; Read, B. E.; Stein, R. S. *J. Phys. Chem.* **1968**, *72*, 1122−1126. (c) Baranovsky, V. Y.; Kotlyarsky, I. V. *Eur. Polym. J.* **1992**, *28*, 1427−1432. (d) Nishi, S.; Kotaka, T. *Macromolecules* **1985**, *18*, 1519−1525.

(20) Wu, C. *Macromolecules* **1994**, *27*, 298−299. (b) Wu, C. *Macromolecules* **1994**, *27*, 7099−7102. (c) Wu, C.; Akashi, M.; Chen, M. Q. *Macromolecules* **1997**, *30*, 2187−2189.

(21) Chen, W. Y.; Zheng, J. X.; Cheng, S. Z. D.; Li, C. Y.; Huang, P.; Zhu, L.; Xiong, H.; Ge, Q.; Guo, Y.; Quirk, R. P.; Lotz, B.; Deng, L.; Wu, C.; Thomas, E. *Phys. Rev. Lett.* **2004**, *93*, 028301-1.

(22) Rangelov, S.; Almgren, M.; Edwards, K.; Tsvetanov, C. *J. Phys. Chem. B* **2004**, *108*, 7542−7552. (b) Zhou, Y.; Yan, D. *Angew. Chem., Int. Ed.* **2005**, *44*, 3223−3226.

(23) Quintana, J. R.; Salazar, R. A.; Katime, I. *J. Phys. Chem.* **1995**, *99*, 3723−3731.

MA0603579